Chinese Journal of Natural Medicines

Anti-inflammatory and hepatoprotective triterpenoids from the traditional Mongolian medicine *Gentianopsis barbata*

Huizhen Cheng, Huan Liu, Xiaoyu Qi, Yuzhou Fan, Zhongzhu Yuan, Yuanliang Xu, Yanchun Liu, Yan Liu, Kai Guo, Shenghong Li

Citation: Huizhen Cheng, Huan Liu, Xiaoyu Qi, Yuzhou Fan, Zhongzhu Yuan, Yuanliang Xu, Yanchun Liu, Yan Liu, Kai Guo, Shenghong Li, Anti-inflammatory and hepatoprotective triterpenoids from the traditional Mongolian medicine *Gentianopsis barbata*, Chinese Journal of Natural Medicines, 2025, 23(9), 1111-1121. doi: 10.1016/S1875-5364(25)60870-3.

View online: https://doi.org/10.1016/S1875-5364(25)60870-3

Chinese Journal of Natural Medicines 23 (2025) 1111-1121

Contents lists available at ScienceDirect

Chinese Journal of Natural Medicines

journal homepage: www.cjnmcpu.com/

Original article

Anti-inflammatory and hepatoprotective triterpenoids from the traditional Mongolian medicine *Gentianopsis barbata*

Huizhen Cheng[a,Δ], Huan Liu[a,Δ], Xiaoyu Qi[a], Yuzhou Fan[a], Zhongzhu Yuan[a], Yuanliang Xu[a], Yanchun Liu[b], Yan Liu[a], Kai Guo[a,*], Shenghong Li[a,b,*]

[a] *State Key Laboratory of Southwestern Chinese Medicine Resources, and Innovative Institute of Chinese Medicine and Pharmacy, Chengdu University of Traditional Chinese Medicine, Chengdu 611137, China*

[b] *State Key Laboratory of Phytochemistry and Plant Resources in West China, and Yunnan Key Laboratory of Natural Medicinal Chemistry, Kunming Institute of Botany, Chinese Academy of Sciences, Kunming 650201, China*

ARTICLE INFO

Article history:
Received 23 September 2024
Revised 3 November 2024
Accepted 28 November 2024
Available online 20 September 2025

Keywords:
Gentianopsis barbata
Gentianaceae
Triterpenoids
Anti-inflammatory activity
Hepatoprotective activity

ABSTRACT

Gentianopsis barbata (*G. barbata*) represents a significant plant species with considerable ornamental and medicinal value in China. This investigation sought to elucidate the primary constituents within the plant and investigate their pharmacological properties. Fifty triterpenoids (**1**–**50**), including nine previously undescribed compounds (**1**, **2**, **7**, **10**, **20**, **28**, **29**, **37**, and **41**) were isolated and characterized from the whole plants of *G. barbata*. Notably, compounds **1** and **2** exhibited the novel 3,4;9,10-*diseco*-24-*homo*-cycloartane triterpenoid skeleton. The isolated triterpenoids demonstrated substantial anti-inflammatory activity through inhibition of tumor necrosis factor α (TNF-α) and interleukin-6 (IL-6) cytokine secretion in LPS-induced RAW264.7 macrophages, and hepatoprotective effects by preventing *tert*-butyl hydroperoxide (*t*-BHP)-induced oxidative injury in HepG2 cells. These results demonstrate both the presence of diverse triterpenoids in *G. barbata* and their therapeutic potential for inflammatory and hepatic conditions, providing scientific evidence supporting the clinical application of this traditional Mongolian medicinal plant.

1. Introduction

Triterpenoids, biosynthesized from the linear precursor 2,3-oxidosqualene (OS) through catalyzation by OS cyclases, represent a major class of plant metabolites widely distributed throughout the plant kingdom. These compounds are notable for their exceptional structural diversity and numerous biological functions (immunomodulatory, anti-oxidant, hypolipidemic, antimicrobial, flavor-altering, etc.) [1]. Triterpenoids occur in plants either in free form or as esters and glycosidic conjugates, such as oleanolic acid in olive fruits and leaves, ursolic acid in apples and bilberries, and ginsenosides in *Panax ginseng* and *P. notoginseng*, where they may consist up to 20% of the dry weight of the separate origin [2, 3]. These natural compounds have been consumed by humans across various cultures and animals worldwide through plant-based foods for centuries, owing to their accessibility and diverse biological roles [4]. Consequently, research examining the cosmeceutical, nutraceutical, and medicinal applications of triterpenoids has grown exponentially, particularly focusing on compounds derived from economically valuable and pharmaceutical plants [5]. This highlights the importance of systematically investigating the unexplored chemical and biological diversity of triterpenoids from valuable plant sources.

Gentianopsis barbata (*G. barbata*) (Froel.) Ma, an annual or biennial grassland herb belonging to the Gentianaceae family, grows at elevations between 700 and 4400 m across Europe, Asia, and North America, demonstrating extensive global distribution primarily in the North Temperate Zone. Beyond its significance as a grassland fodder plant, *G. barbata* possesses considerable ornamental value due to its distinctive bright purple flowers [6]. In traditional Mongolian medicine, the whole plants of *G. barbata* serve as a treatment for liver and bile diseases [7]. While numerous studies have examined the phytochemicals of Gentianaceae plants, investigations specific to *G. barbata* remain limited, with only one triterpenoid (oleanolic acid), three monoterpene glycosides, and several xanthones identified to date [7, 8]. The molecular basis for the traditional therapeutic applications of *G. barbata* remains incompletely understood. This study presents a comprehensive phytochemical analysis of the methanol extract from *G. barbata* whole plants, yielding the isolation and characterization of triterpenoids (**1**–**50**, Fig. 1). Nine novel compounds (**1**, **2**, **7**, **10**, **20**, **28**, **29**, **37**, and **41**) were identified, with **1** and **2** exhibiting a novel 3,4;9,10-*diseco*-24-*homo*-cycloartane skeleton. The anti-inflammatory and hepatoprotective properties of these triterpenoid isolates were subsequently evaluated. The following sections detail the findings of this investigation.

* Corresponding author.
E-mail addresses: guokai@cdutcm.edu.cn (K. Guo); shli@mail.kib.ac.cn (S. Li)
Δ These authors contributed equally to this work.

https://doi.org/10.1016/S1875-5364(25)60870-3

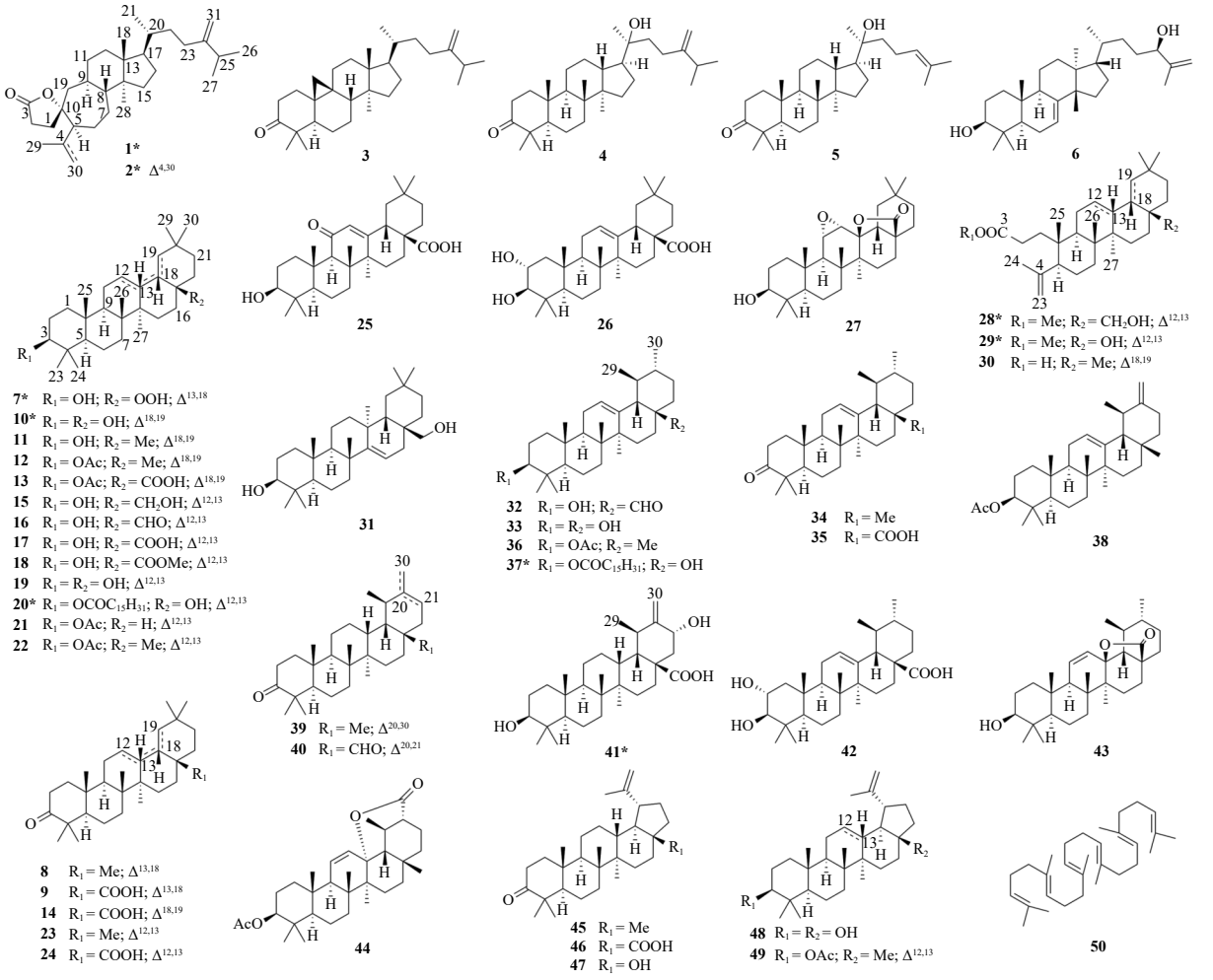

Fig. 1 Structures of triterpenoids **1**–**50** isolated from *G. barbata* (new compounds were marked with asterisk).

2. Results and discussion

2.1. Structural elucidation

Compound **1** was isolated as white powder and exhibited the molecular formula $C_{31}H_{52}O_2$ based on its high-resolution electrospray ionization mass spectrometry (HR-ESI-MS) (*m/z* 479.3861 $[M + Na]^+$, Calcd. 479.3860). The ^{13}C nuclear magnetic resonance (NMR) (DEPT) spectra of **1** (Table 1) revealed 31 carbon resonances attributed to seven methyls, twelve methylenes (including an olefinic at δ_C 106.1), seven methines, and five quaternary carbons (including an oxygenated at δ_C 93.2, an olefinic at δ_C 157.0, and a keto at δ_C 177.4). The ^1H NMR spectrum (Table 2) distinctly showed five secondary methyls at δ_H 1.03 (d, *J* = 6.8 Hz), 1.02 (d, *J* = 6.8 Hz), 0.92 (d, *J* = 6.8 Hz), and 0.89 (d, *J* = 6.5 Hz, 2 × CH_3), two tertiary methyls at δ_H 0.84 (s) and 0.81 (s), and a pair of terminal olefinic protons at δ_H 4.71 (br s) and 4.66 (br s). These spectral characteristics indicated **1** to be a *homo*-triterpenoid. Analysis of the HSQC spectrum of **1** enabled assignment of all proton signals to their corresponding carbons. The ^1H–^1H correlation spectroscopy (COSY) relationships of H_3-29(H_3-30)/H-4/H-5/H_2-6/H_2-7/H-8/H-9/H_2-19 and H_2-1/H_2-2, and the heteronuclear multiple bond correlation (HMBC) from H_2-1 to C-3/C-5/C-19, H_2-2 to C-10, and H_2-6/H-9 to C-10 (Fig. 2), combined with the molecular formula of **1** and the deshielded chemical shifts of C-3 (δ_C 177.4) and C-10 (δ_C 93.2), established a spiro structure fused by a butyrolactone and a cycloheptane ring with an isopropyl unit. Based on this, further examination of the additional ^1H–^1H COSY relationships of H-8/H-9/H_2-11/H_2-12, H_2-15/H_2-16/H-17/H-20/H_2-22(H_3-21)/H_2-23, and H_3-26/H-25/H_3-27, along with the key HMBC from H_3-28 to C-8/C-13/C-15, H_3-18 to C-12/C-14/C-17, H_3-21 to C-17/C-22, and H_2-31 to C-23/C-25, conclusively elucidated the planar structure of **1** with a 5/7/6/5 ring system. The nuclear Overhauser effect spectroscopy (NOESY) correlations (Fig. 2) of H_2-1 with H-8, H-9 with H-5/H_3-28, H-8 with H_3-18, and H-17 with H_3-28 determined the relative configuration of the ring system. Although suitable crystals of **1** were unavailable despite numerous attempts, a single crystal of 3-oxo-24-methylenecycloarane (**3**), a known triterpenoid also isolated in this study, was successfully obtained. Single crystal X-ray diffraction analysis confirmed the absolute configuration of **3** (Fig. 3). Given that **1** likely derives from the enzyme-catalyzed cleavage of **3**, and their nearly identical chemical shifts of the C-17 side chain, the remaining C-20 configuration of **1** was tentatively assigned identical to **3**. The calculated electronic circular dichroism (ECD) results (Fig. 4) demonstrated good agreement between the calculated and experimental curves of **1**, establishing the absolute configuration of **1** as depicted in Fig. 1. Consequently, the structure of **1** (trivially named gentianopsolide A), featuring a novel 3,4;9,10-*diseco*-24-*homo*-cycloartane skeleton, was established.

Compound **2**, isolated as a white powder, exhibited a molecular formula $C_{31}H_{50}O_2$ based on HR-ESI-MS analysis (*m/z* 455.3885 $[M + H]^+$). The ^1H and ^{13}C NMR spectral data of **2** showed close similarity to those of **1** (Tables 1 and 2), suggesting analogous chemical structures. The primary distinction was the replacement of the C-30 methyl (δ_H 0.89; δ_C 18.7) and C-4

Table 1 ^{13}C NMR spectroscopic data for compounds.

No.	**1**[a]	**2**[a]	**7**[a]	**10**[a]	**20**[a]	**28**[a]	**29**[a]	**37**[a]	**41**[b]
1	30.3 CH_2	31.7 CH_2	39.0 CH_2	39.0 CH_2	38.2 CH_2	34.0 CH_2	33.9 CH_2	38.4 CH_2	40.1 CH_2
2	29.9 CH_2	29.8 CH_2	27.5 CH_2	27.4 CH_2	23.7 CH_2	28.5 CH_2	28.5 CH_2	23.7 CH_2	27.9 CH_2
3	177.4 C	177.5 C	79.1 CH	79.0 CH	80.7 CH	174.6 C	174.6 C	80.7 CH	79.7 CH
4	27.6 CH	146.8 C	40.0 C	38.9 C	37.9 C	147.4 C	147.4 C	37.9 C	40.0 C
5	51.8 CH	54.9 CH	55.5 CH	55.5 CH	55.4 CH	50.4 CH	50.4 CH	55.4 CH	57.0 CH
6	23.7 CH_2	29.7 CH_2	18.7 CH_2	18.2 CH_2	18.4 CH_2	24.5 CH_2	27.3 CH_2	18.3 CH_2	19.4 CH_2
7	32.1 CH_2	30.7 CH_2	34.2 CH_2	34.6 CH_2	32.8 CH_2	31.3 CH_2	31.5 CH_2	33.1 CH_2	35.2 CH_2
8	48.6 CH	48.6 CH	42.5 C	40.7 C	39.8 C	39.5 C	39.2 C	40.0 C	42.1 C
9	31.4 CH	31.8 CH	51.6 CH	51.2 CH	47.7 CH	37.8 CH	37.9 CH	47.7 CH	52.1 CH
10	93.2 C	91.9 C	37.6 C	37.2 C	37.1 C	39.1 C	39.3 C	37.0 C	38.3 C
11	31.7 CH_2	31.6 CH_2	22.7 CH_2	21.0 CH_2	23.8 CH_2	23.7 CH_2	24.5 CH_2	23.7 CH_2	22.7 CH_2
12	32.8 CH_2	32.8 CH_2	27.4 CH_2	25.8 CH_2	124.5 CH	122.3 CH	124.1 CH	127.9 CH	28.1 CH_2
13	45.6 C	45.6 C	128.3 C	38.2 CH	143.4 C	144.1 C	143.2 C	138.1 C	39.9 CH
14	49.2 C	49.4 C	48.4 C	42.6 C	41.7 C	42.3 C	42.1 C	42.0 C	42.8 C
15	33.5 CH_2	33.5 CH_2	28.9 CH_2	27.0 CH_2	25.6 CH_2	25.5 CH_2	25.4 CH_2	26.1 CH_2	29.0 CH_2
16	28.0 CH_2	28.0 CH_2	38.0 CH_2	36.4 CH_2	27.5 CH_2	22.0 CH_2	33.8 CH_2	28.6 CH_2	35.4 CH_2
17	51.0 CH	51.0 CH	102.5 C	68.3 C	72.3 C	36.9 C	72.2 C	72.3 C	48.0 C
18	14.8 CH_3	14.8 CH_3	141.3 C	139.7 C	48.9 C	42.4 CH	48.8 CH	60.7 C	50.5 CH
19	49.6 CH_2	49.3 CH_2	44.7 CH_2	133.1 CH	48.4 CH_2	46.4 CH_2	48.3 CH_2	41.7 CH	41.0 CH
20	36.3 CH	36.3 CH	33.3 C	32.4 C	31.2 C	30.9 C	31.0 C	39.4 CH	154.5 C
21	18.5 CH_3	18.7 CH_3	35.6 CH_2	32.9 CH_2	36.6 CH_2	34.1 CH_2	36.5 CH_2	40.5 CH_2	72.2 CH
22	35.1 CH_2	35.1 CH_2	37.0 CH_2	36.4 CH_2	36.9 CH_2	31.0 CH_2	36.9 CH_2	32.5 CH_2	46.4 CH_2
23	31.4 CH_2	31.4 CH_2	15.5 CH_3	15.4 CH_3	28.2 CH_3	113.6 CH_2	113.6 CH_2	28.3 CH_3	28.6 CH_3
24	157.0 C	157.0 C	28.1 CH_3	28.0 CH_3	16.9 CH_3	23.6 CH_3	23.5 CH_3	17.0 CH_3	16.1 CH_3
25	33.9 CH	33.9 CH	16.5 CH_3	16.7 CH_3	15.5 CH_3	19.5 CH_3	19.4 CH_3	15.7 CH_3	16.9 CH_3
26	22.0 CH_3	22.0 CH_3	17.0 CH_3	16.2 CH_3	17.2 CH_3	16.8 CH_3	17.2 CH_3	17.3 CH_3	16.6 CH_3
27	22.1 CH_3	22.1 CH_3	21.1 CH_3	14.2 CH_3	25.6 CH_3	25.7 CH_3	25.3 CH_3	23.2 CH_3	14.1 CH_3
28	16.8 CH_3	16.9 CH_3			32.9 CH_3	69.7 CH_2		17.5 CH_3	179.7 C
29	23.7 CH_3	22.8 CH_3	32.8 CH_3	30.9 CH_3	24.1 CH_3	23.5 CH_3	23.9 CH_3	20.9 CH_3	27.7 CH_3
30	18.7 CH_3	115.2 CH_2	25.4 CH_3	27.6 CH_3		33.2 CH_3	32.7 CH_3		116.5 CH_2
31	106.1 CH_2	106.1 CH_2							
1’					173.9 C			173.9 C	
2’					35.0 CH_2			35.0 CH_2	
3’					25.3 CH_2			25.3 CH_2	
4’-13’					29.3-29.9 CH_2			29.3-29.9 CH_2	
14’					32.1 CH_2			32.1 CH_2	
15’					22.9 CH_2			22.9 CH_2	
16’					14.3 CH_3			14.3 CH_3	
OMe						51.6 CH_3	51.6 CH_3		

[a] ^{13}C NMR (150 MHz) in $CDCl_3$; [b] ^{13}C NMR (150 MHz) in CD_3OD.

Table 2 ^{1}H NMR spectroscopic data for compounds **1**, **2**, **7**, **10**, and **41.**

No.	**1**[a]	**2**[a]	**7**[a]	**10**[a]	**41**[b]
1a	2.39 m	2.34 m	1.69 m	1.75 m	1.64 m
1b	1.17 m	1.75 m	0.97 m	0.94 m	0.88 m
2a	2.62 m	2.47 m	1.63 m	1.64 m	1.67 m
2b	2.53 m	2.46 m	1.58 m	1.59 m	1.49 m
3			3.21 dd (11.5, 4.7)	3.21 m	3.04 m
4	1.80 m				
5	1.73 m	2.57 dd (9.6, 2.3)	0.72 m	0.70 br d (11.9)	0.63 m
6a	1.60 m	1.76 m	1.55 m	1.52 m	1.44 m
6b	1.12 m	1.50 m	1.38 m	1.37 m	1.31 m
7a	1.72 m	1.66 m	1.51 m	1.50 m	1.64 m
7b	1.34 m	1.45 m	1.27 m	1.33 m	1.36 m
8	1.44 m	1.45 m			
9	1.84 m	1.91 m	1.48 m	1.27 m	1.30 m
11a	1.45 m	1.46 m	1.52 m	1.56 m	1.52 m
11b	1.29 m	1.32 m	1.27 m	1.27 m	1.23 m
12a	1.63 m	1.63 m	2.19 m	1.53 m	1.54 m
12b	1.51 m	1.53 m	1.99 m	1.16 m	0.98 m
13				2.50 br d (12.4)	2.53 m
15a	1.25 m	1.22 m	2.53 m	1.95 m	1.46 m
15b	1.21 m	1.21 m	1.11 m	1.12 m	1.00 m
16a	1.92 m	1.92 m	2.01 m	1.66 m	1.30 m
16b	1.28 m	1.29 m	2.00 m	1.50 m	
17	1.54 m	1.55 m			
18	0.81 s	0.81 s			1.14 m
19a	1.75 m	1.81 m	2.36 d (12.8)	5.04 s	2.38 m
19b	1.66 m	1.69 m	1.79 d (12.8)		
20	1.42 m	1.41 m			
21a	0.89 d (6.5)	0.90 d (6.5)	1.66 m	1.47 m	4.24 dd (9.2, 6.0)
21b			1.16 m	1.38 m	
22a	1.56 m	1.56 m	1.98 m	1.69 m	2.52 m
22b	1.13 m	1.13 m	1.78 m	1.56 m	1.18 m
23a	2.11 m	2.11 m	0.76 s	0.77 s	0.86 s
23b	1.89 m	1.88 m			
24			0.97 s	0.97 s	0.66 s
25	2.23 m	2.23 m	0.85 s	0.88 s	0.79 s
26	1.03 d (6.8)	1.03 d (6.8)	1.05 s	1.09 s	0.91 s
27	1.02 d (6.8)	1.02 d (6.8)	1.14 s	0.74 s	0.88 s
28	0.84 s	0.84 s			
29	0.92 d (6.8)	1.78 s	0.97 s	0.99 s	1.14 s
30a	0.89 d (6.5)	4.93 br s	0.82 s	0.94 s	4.81 br s
30b		4.82 br s			4.73 br s
31a	4.71 br s	4.71 br s			
31b	4.66 br s	4.66 br s			

[a] ^{1}H NMR (700 MHz) in $CDCl_3$; [b] ^{1}H NMR (700 MHz) in CD_3OD.

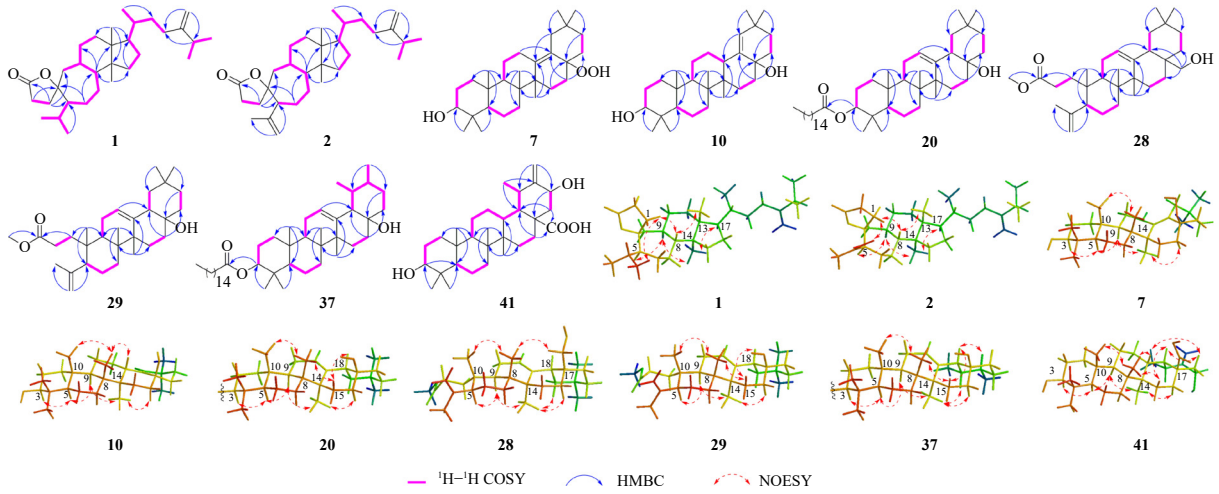

Fig. 2 Key ^{1}H–^{1}H COSY, HMBC and ROESY correlations of the new compounds.

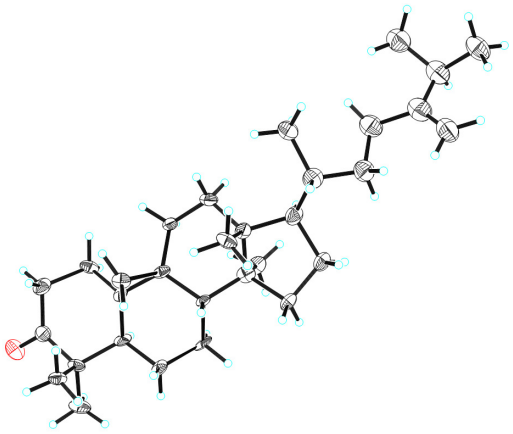

Fig. 3 X-ray crystallographic structure of compound **3**.

methine (δ_H 1.80; δ_C 27.6) in **1** with a terminal double bond (δ_H 4.93, 4.82; δ_C 146.8, 115.2), evidenced by key HMBC from H_2-30 to C-5/C-29 (Fig. 2). The relative configuration of **2** was established through key NOESY correlations of H_2-1 with H-8, H-9 with H-5/H_3-28, H-8 with H_3-18, and H-17 with H_3-28 (Fig. 2), supported by consistent NMR data and probable shared biosynthetic pathways of **1**–**3**. The absolute configuration of **2** was determined through calculated ECD analysis (Fig. 4). Thus, compound **2** was designated as gentianopsolide B.

Compound **7**, obtained as white powder, displayed a molecular formula $C_{29}H_{48}O_3$ through HR-EI-MS analysis (*m/z* 444.3597 [M]+). Comparison of ^{1}H and ^{13}C NMR data between **7** and 3-oxo-olean-13(18)-en-28-oic acid (**9**) [9], a previously documented triterpenoid also isolated in this study, revealed significant structural similarities. The notable difference was the absence of downfield ketos (C-3: δ_C 218.3; C-28: δ_C 179.7) in **7**, replaced by an oxygenated methine (δ_H 3.21; δ_C 79.1). Additionally, the C-17 quaternary carbon shifted significantly downfield from **9** (δ_C 50.1) to **7** (δ_C 102.5), indicating the presence of a perhydroxyl group. The ^{1}H–^{1}H COSY correlation of H-3/H_2-2/H_2-1 and HMBC from H-3 to C-1/C-5 and H_2-15/H_2-19/H_2-21 to C-17 (Fig. 2) confirmed the hydroxyl and perhydroxyl group positions at C-3 and C-17, respectively. The *β*-configuration of 3-OH and relative configurations of **7** were established through the large coupling constant of H-3 (δ_H 3.21, dd, *J* = 11.5, 4.7 Hz) and key NOESY correlations of H-5 with H-3/H-9, H_3-25 with H_3-26, and H_3-27 with H-9/H_2-16 (Fig. 2). The *β*-configuration of 17-OOH was supported by ^{1}H and ^{13}C NMR calculations using DP4+ analysis (Table S10). The absolute configuration of **7** was determined through ECD calculations(Fig. 4). Compound **7** was thus named 17*β*-hydroperoxide olean-13(18)-en-3*β*-ol.

Compound **10** was isolated as white powder, with a molecular formula $C_{29}H_{48}O_2$ based on the HR-ESI-MS (*m/z* 451.3548 [M + Na]$^+$). The ^{1}H and ^{13}C NMR data of **10** (Tables 1 and **10**) exhibited strong similarities to those of germanicol (**11**) [10], a known triterpenoid also isolated in this study. The primary distinction was the absence of the C-28 methyl (δ_H 0.97; δ_C 25.4) in **10**, while the C-17 quaternary carbon (δ_C 34.5) of **11** displayed a downfield shift (δ_C 68.3) in **10**. This, combined with the molecular weight of **10** and the HMBC from H_2-15/H-19/H_2-21 to C-17 (Fig. 2), confirmed the presence of 17-OH. The relative configurations of **10** were determined through key NOESY correlations of H-5 with H-3/H-9, H_3-26 with H-13/H_3-25, and H_3-27 with H-9/H_2-16 (Fig. 2). The ^{1}H and ^{13}C NMR calculations by DP4+ analysis further supported the β-configuration of 17-OH (Table S11). The absolute configuration of **10** was verified through comparison of calculated and experimental ECD curves (Fig. 4). Compound **10** was consequently named 28-*nor*-olean-18-en-3*β*,17*β*-diol.

Compound **20**, obtained as white powder, possessed the molecular formula $C_{45}H_{78}O_3$ according to its HR-ESI-MS (*m/z* 689.5836 [M + Na]$^+$). The ^{1}H and ^{13}C NMR data (Tables 1 and 3) of **20** showed marked similarity to those of 28-*nor*-olean-12-en-3*β*,17*β*-diol (**19**) [11], a known triterpenoid also identified in this study. The notable difference was the presence of a palmitoyl group [δ_H 0.88, 1.25–1.30, 1.62, 2.29; δ_C 173.9, 35.0, 25.3, 29.3–29.9 (10 × CH_2), 32.1, 22.9, 14.3] in **20**. The key HMBC from H-3 to C-1' and the characteristic chemical shift resulting from esterification (C-3: δ_C 80.7 for **20**, δ_C 79.0 for **19**) established the C-3 linkage of the palmitoyl in **20**. The configurations of **20** were determined through NOESY correlations of H-5 with H-3/H-9, H-15a with H-18/H_3-26, H_3-25 with H_3-26, and H_3-27 with H-9/H_2-16, supported by NMR calculations using DP4+ analysis (Table S12) and ECD calculations (Fig. 4) determined the configurations of **20**. The compound was named 3*β*-palmitoyl-28-*nor*-olean-12-en-17*β*-ol.

Compound **28**, a white powder, exhibited a molecular formula of $C_{31}H_{50}O_3$ based on HR-EI-MS analysis (*m/z* 470.3756 [M]$^+$). Comparison of the ^{1}H and ^{13}C NMR data (Tables 1 and 3) between **28** and 3,4-*seco*-olean-4(23),18-dien-3-oic acid (**30**) [12], a known triterpenoid also isolated in this study, revealed close structural similarities. The primary distinction was the replacement of the C-28 methyl (δ_H 1.01; δ_C 25.3) in **30** with an oxygenated methylene (δ_H 3.56, 3.22; δ_C 69.7) in **28**, and the presence of an additional methoxyl (δ_H 3.65; δ_C 51.6). HMBC from the methoxyl to C-3 (δ_C 174.6), and H_2-28 to C-16/C-18/C-22 (Fig. 2) confirmed the C-3 position of a methyl ester and the C-28 position of

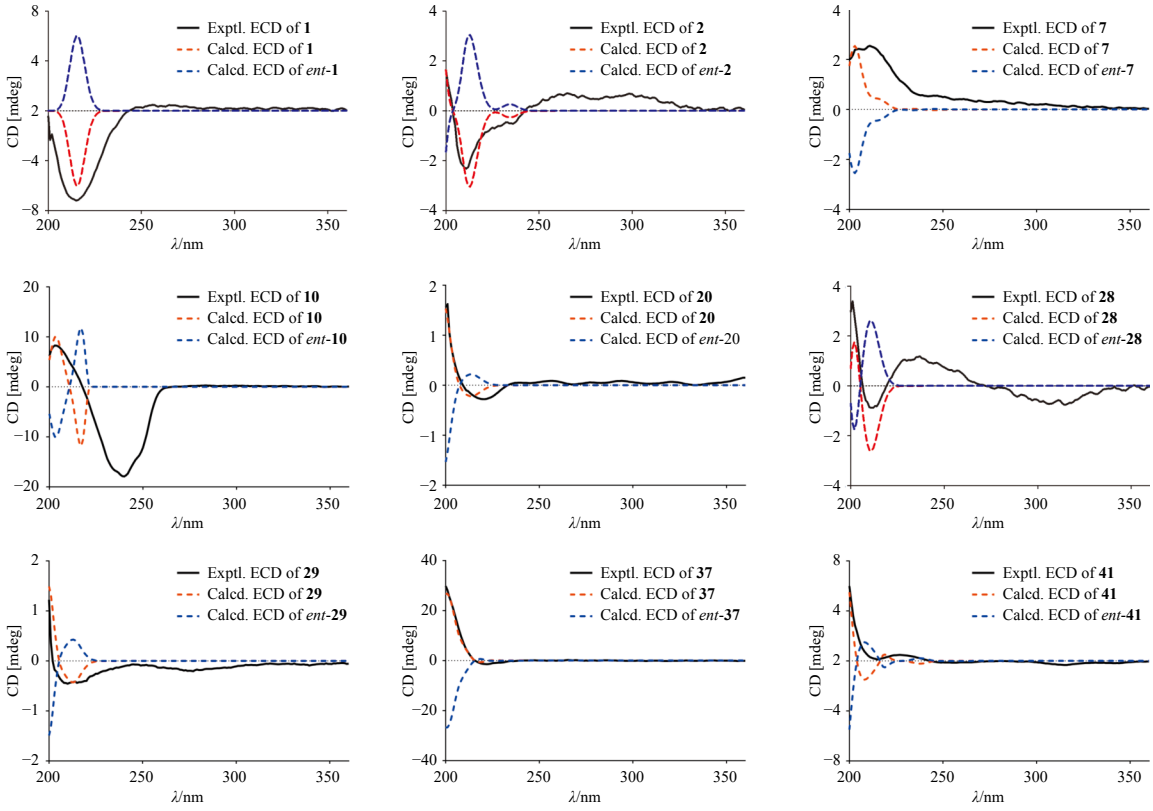

Fig. 4 Experimental and calculated ECD spectra of the new compounds.

a hydroxyl group in **28**. Furthermore, HMBC from H-12 (δ_H 5.21) to C-9/C-14/C-18 and H-18 (δ_H 2.00) to C-12/C-13/C-14, along with the downfield chemical shifts of C-12 (δ_C 122.3, CH) and C-13 (δ_C 144.1, C), indicated the double bond formation at C-12/C-13 in **28** rather than C-18/C-19 in **30**. The configurations of **28** were determined through analysis of NOESY correlations (H-9 with H-5/H_3-27, H_3-26 with H_3-25/H_2-28, and H_3-27 with H_2-19) (Fig. 2) and calculated NMR and ECD results Fig. 4), leading to its designation as gentianopsolide C.

Compound **29**, a white powder, demonstrated a molecular formula of $C_{30}H_{48}O_3$ as determined by HR-EI-MS (*m/z* 456.3597 $[M]^+$). The ^1H and ^{13}C NMR data of **29** exhibited strong similarity to those of **28** (Tables 1 and 3), with the main distinction being the absence of C-28 methylene (δ_H 3.56, 3.22; δ_C 69.7) and the downfield shifted C-17 (δ_C 72.2 for **29**, 36.9 for **28**) in **29**. Analysis of the molecular weight and HMBC from H_2-15/H_2-19/H_2-21 to C-17 in **29** confirmed the presence of 17-OH (Fig. 2). The configurations of **29** were established through NOESY correlations of H-9 with H-5/H_3-27, H-15a with H-18/H_3-26, H_3-26 with H_3-25, and H_3-27 with H_2-16, supported by NMR and ECD calculations (Table S14 and Fig. 4). Compound **29** was subsequently named gentianopsolide D.

Compound **37** was isolated as colorless oil with the molecular formula $C_{45}H_{78}O_3$ determined by HR-ESI-MS (*m/z* 667.6043 $[M + H]^+$). The ^1H and ^{13}C NMR spectral data (Tables 1 and 3) of **37** exhibited close similarity to those of 28-*nor*-urs-12-en-3*β*,17*β*-diol (**33**) [13], a known triterpenoid also isolated in this study. The primary distinction was the presence of an additional palmitoyl group [δ_H 0.88, 1.25–1.30, 1.62, 2.29; δ_C 173.9, 35.0, 25.3, 29.3–29.9 (10 × CH_2), 32.1, 22.9, 14.3] in **37**. The key HMBC from H-3 to C-1' and the characteristic chemical shift induced by esterification (C-3: δ_C 80.7 for **37**, δ_C 79.0 for **33**) confirmed the C-3 attachment of the palmitoyl group in **37** (Fig. 2). The NOESY correlations of H-5 with H-3/H-9, H-9 with H_3-27, H-15a with H-18/H_3-26, H_3-26 with H_3-25, H-20 with H-18, and H_3-27 with H-19/H_2-16 (Fig. 2), combined with the calculated NMR and ECD results (Table S15 and Fig. 4) assigned the configurations of **37**, which was named 3*β*-palmitoyl-28-*nor*-urs-12-en-17*β*-ol.

Compound **41**, obtained as white powder, was determined to have the molecular formula $C_{30}H_{47}O_4$ based on HR-ESI-MS (*m/z* 471.3484 $[M - H]^-$). Comprehensive analysis of its 1D and 2D NMR data (Tables 1 and 2) compared with those of taraxasterone (**39**) [14], a known triterpenoid also isolated in this investigation, indicated that the C-3 keto, C-21 methylene, and C-28 methyl of **39** were replaced in **41** by two oxygenated methines (δ_H 3.04, δ_C 79.7; δ_H 4.24, δ_C 72.2) and a carboxyl (δ_C 179.7). The HMBC from H-3 (δ_H 3.04) to C-1/C-5/C-23, H-21 (δ_H 4.24) to C-17/C-19/C-30, and H_2-16/H-18/H_2-22 to C-28 confirmed the positions of 3-OH, 21-OH, and 17-COOH, respectively (Fig. 2). The relative configuration of **41** was determined through analysis of NOESY correlations of H-5 with H-3/H-9, H-9 with H_3-27, H_3-26 with H_3-25/H-13, H-15a with H-18/H_3-26, H_3-27 with H_2-16, and H-21 with H-18/H_3-29 (Fig. 2), while the calculated NMR results (Table S16) further supported the *β*-configuration of the carboxyl group. The absolute configuration of **41** was established through calculated ECD results (Fig. 4), and compound **41** was consequently named urs-20(30)-en-3*β*,21*α*-diol-28-oic acid.

The remaining 41 triterpenoid isolates were identified through comparison of their spectroscopic data with published literature values as: 3-oxo-24-methylenecycloarane (**3**) [15], vellozone (**4**) [16], dipterocarpol (**5**) [17], (24*R*)-eupha-7,25-dien-3*β*,24-diol (**6**) [18], olean-13(18)-en-3-one (**8**) [19], 3-oxo-olean-13(18)-en-28-oic acid (**9**) [9], geramanicol (**11**) [10], germanicol acetate (**12**) [20], morolic acid acetate (**13**) [21], moronic acid (**14**) [22], erythrodiol (**15**) [23], olean-12-en-3*β*-ol-28-al (**16**) [19], oleanolic acid (**17**) [24], methyl oleanolate (**18**) [21], 28-*nor*-olean-12-en-3*β*,17*β*-diol (**19**) [11], 3*β*-acetoxy-28-*nor*-olean-12-ene (**21**) [20], *β*-amyrin acetate (**22**) [24], olean-12-en-3-one (**23**) [14], 3-oxo-oleanolic acid (**24**) [25], 11-oxo-oleanolic acid (**25**) [25], olean-12-en-2*α*,3*β*-diol-28-oic acid (**26**) [26], 3*β*-hydroxy-11*α*,12*α*-epoxyoleanan-28,13*β*-olide (**27**) [27], 3,4-*seco*-olean-4(23),18- dien-3-oic acid (**30**) [12], myricadoil (**31**) [28], ursaldehyde (**32**) [25], 28-*nor*-urs-12-en-3*β*,17*β*-diol

Table 3 ^{1}H NMR spectroscopic data for compounds **20**, **28**, **29**, and **37**.

No.	**20**[a]	**28**[a]	**29**[a]	**37**[a]
1a	1.62 m	1.58 m	1.58 m	1.65 m
1b	1.06 m			1.09 m
2a	1.63 m	2.37 m	2.38 m	1.63 m
2b	1.62 m	2.21 m	2.22 m	1.63 m
3	4.51 m			4.51 m
5	0.86 m	1.97 m	1.97 m	0.85 m
6a	1.55 m	1.78 m	2.04 m	1.54 m
6b	1.42 m	1.40 m	1.19 m	1.41 m
7a	1.50 m	1.53 m	1.51 m	1.54 m
7b	1.39 m	1.31 m	1.40 m	1.41 m
9	1.58 m	1.77 m	1.77 m	1.56 m
11a	1.90 m	1.94 m	1.79 m	1.95 m
11b	1.89 m	1.81 m	1.41 m	1.94 m
12	5.31 t (4.0)	5.21 m	5.32 m	5.31 t (4.0)
15a	1.99 m	1.71 m	1.99 m	2.03 m
15b	1.04 m	1.03 m	1.08 m	1.06 m
16a	2.05 m	1.90 m	1.98 m	2.03 m
16b	1.18 m	1.18 m	1.82 m	1.25 m
18	2.23 m	2.00 m	2.23 m	1.58 m
19a	1.63 m	1.73 m	1.63 m	1.27 m
19b	1.20 m	1.08 m	1.20 m	
20				0.98 m
21a	1.29 m	1.30 m	1.30 m	1.73 m
21b	1.29 m	1.19 m		1.54 m
22a	1.69 m	1.54 m	1.70 m	1.58 m
22b	1.51 m	1.35 m	1.51 m	1.18 m
23a	0.87 s	4.87 br s	4.88 br s	0.87 s
23b		4.67 br s	4.71 br s	
24	0.88 s	1.75 s	1.75 s	0.88 s
25	0.95 s	0.94 s	0.94 s	0.98 s
26	0.96 s	1.00 s	1.01 s	1.00 s
27	1.14 s	1.18 s	1.15 s	1.08 s
28a		3.56 d (9.1)		
28b		3.22 d (9.1)		
29	0.90 s	0.88 s	0.90 s	0.83 d (6.5)
30a	0.96 s	0.89 s	0.98 s	0.93 d (6.3)
2'	2.29 m			2.29 m
3'	1.62 m			1.62 m
4'-13'	1.25-1.30 m			1.25-1.30 m
14'	1.25 m			1.25 m
15'	1.29 m			1.29 m
16'	0.88 t (7.0)			0.88 t (7.0)
OMe		3.65 s	3.65 s	

[a] ^{1}H NMR (700 MHz) in $CDCl_3$.

(**33**) [13], 3-oxo-ursolic acid (**34**) [26], ursonic acid (**35**) [25], *α*-amyrin acetate (**36**) [26], taraxasterol acetate (**38**) [29], taraxasterone (**39**) [14], 3-oxo-urs-20-en-28-al (**40**) [26], urs-12-en-2*α*,3*β*-diol-28-oic acid (**42**) [26], urs-11-en-3*β*-ol-28,13*β*-olide (**43**) [26], 3*β*-acetoxy-urs-11-en-13*α*,30-olide (**44**) [30], lupenone (**45**) [26], betulonic acid (**46**) [26], 28-*nor*-lup-20(29)-en-17*β*-ol-3-one (**47**) [26], 28-*nor*-lup-20(29)-en-3*β*,17*β*-diol (**48**) [26], 3*β*-acetoxy-lup-12,20(30)-diene (**49**) [31], and squalene (**50**) [32].

This study represents the most comprehensive investigation of triterpenoid components in Gentianaceae plants to date. A total of 50 triterpenoids comprising 15 distinct chemical skeletons were identified from *G. barbata*. Compounds **1** and **2** feature a novel 3,4;9,10-*diseco*-24-*homo*-cycloartane scaffold, while the remaining 14 known triterpenoid skeletons include 24-*homo*-cycloartane (**3**), 24-*homo*-dammarane (**4**), dammarane (**5**), euphane (**6**), oleanane (**8**, **9**, **11**–**18**, and **22**–**27**), 28-*nor*-oleanane (**7**, **10**, and **19**–**21**), 3,4-*seco*-oleanane (**28** and **30**), 3,4-*seco*-28-*nor*-oleanane (**29**), 27(14→13)-*abeo*-oleanane (**31**), ursane (**32**, **34**–**36**, and **38**–**44**), 28-*nor*-ursane (**33** and **37**), lupane (**45**, **46**, and **49**), 28-*nor*-lupane (**47** and **48**), and the linear triterpene (**50**). These findings demonstrate the significant capacity of Gentianaceae plants to produce diverse triterpenoid metabolites.

2.2. Anti-inflammatory activity

Recent research has increasingly focused on herbs as natural sources of anti-inflammatory agents. Triterpenoids represent a major class of natural anti-inflammatory compounds in plants, with well-documented bioactivity [5]. This study evaluated the anti-inflammatory effects of the isolated triterpenoids by measuring their inhibition of tumor necrosis factor α (TNF-α) and interleukin-6 (IL-6) secretion in LPS-induced macrophages RAW264.7. The analysis revealed that 19 compounds (**3**, **5**, **6**, **14**, **19**, **22**, **25**, **28**–**31**, **37**, **38**, **40**, **42**–**44**, **47**, and **50**) exhibited substantial inhibitory activity against TNF-α secretion, with half maximal inhibitory concentration (IC_{50}) values between 1.56 and 8.07 μmol·L^{-1} (Table 4). Additionally, 12 compounds (**5**, **14**, **22**, **25**, **28**–**31**, **37**, **38**, **44**, and **50**) demonstrated significant inhibitory activity against IL-6 secretion, with IC_{50} values ranging from 3.65 to 22.31 μmol·L^{-1} (Table 4). Analysis of structure-activity relationships revealed several patterns: 24-*homo*-dammarane exhibits lower activity than normal dammarane (**4** *vs* **5**), while 3,4-*seco*-oleanane and 27(14→13)-*abeo*-oleanane show higher activity than normal oleanane (**28** *vs* **15**, **30** *vs* **11**, and **31** *vs* **15**). In normal oleanane structures, a C-18/C-19 double bond (**14**) appears more beneficial for activity compared to C-13/18 (**9**) or C-12/C-13 (**24**) double bonds. The removal of 28-Me significantly reduces oleanane activity (**22** *vs* **21**). For 28-*nor*-ursane, a palmitoyl group at C-3 notably enhances activity (**37** *vs* **33**). Furthermore, substituting 28-Me with a hydroxyl in lupane (**45** vs **47**) improves activity. These results establish diverse triterpenoids as key chemical constituents of *G. barbata* with anti-inflammatory properties, providing a foundation for developing novel immunosuppressants.

2.3. Hepatoprotective activity

Based on the traditional clinical applications of *G. barbata* in treating liver diseases, the hepatoprotective activity of these triterpenoid isolates was investigated. *Tert*-butyl hydroperoxide (*t*-BHP), which metabolizes into harmful free radical intermediates, serves as a widely accepted model for inducing hepatotoxicity in HepG2 cells [33]. The protective effects of the isolated triterpenoids (**1**–**50**) against *t*-BHP-induced hepatotoxicity in HepG2 cells were evaluated at 20 μmol·L^{-1}. The results (Fig. 5) indicated that 30 triterpenoids (**5**–**10**, **12**, **14**, **15**, **17**, **19**, **20**, **22**, **23**, **25**, **26**, **29**–**31**, **33**–**35**, **37**, **38**, **40**–**44**, **48**, and **50**) demonstrated en-

Table 4 Anti-inflammatory activity of the triterpenoid isolates.

No.	TNF-α secretion		IL-6 secretion		No.	TNF-α secretion		IL-6 secretion	
	IR (%, 20 μmol·L^{-1})	IC_{50} (μmol·L^{-1})	IR (%, 20 μmol·L^{-1})	IC_{50} (μmol·L^{-1})		IR (%, 20 μmol·L^{-1})	IC_{50} (μmol·L^{-1})	IR (%, 20 μmol·L^{-1})	IC_{50} (μmol·L^{-1})
1	< 10	–	< 10	–	**27**	28.48 ± 4.15	–	< 10	–
2	< 10	–	< 10	–	**28**	85.63 ± 1.33	1.98 ± 0.62	68.59 ± 2.09	22.31 ± 0.73
3	72.43 ± 0.58	8.07 ± 1.76	36.56 ± 3.04	–	**29**	85.88 ± 2.16	3.16 ± 1.72	79.88 ± 1.75	14.17 ± 1.55
4	23.34 ± 4.10	–	18.63 ± 5.80	–	**30**	91.15 ± 5.95	3.57 ± 0.42	68.53 ± 4.52	14.49 ± 1.17
5	77.03 ± 2.46	5.56 ± 0.44	67.84 ± 1.79	12.70 ± 1.29	**31**	77.49 ± 1.75	4.84 ± 1.46	79.06 ± 0.94	13.48 ± 0.94
6	84.86 ± 1.32	1.97 ± 0.11	36.32 ± 0.38	–	**32**	41.16 ± 3.55	–	< 10	–
7	< 10	–	15.37 ± 5.03	–	**33**	48.10 ± 1.74	–	30.36 ± 3.65	–
8	< 10	–	< 10	–	**34**	46.95 ± 0.98	–	< 10	–
9	19.39 ± 0.64	–	39.13 ± 2.83	–	**35**	54.28 ± 1.98	–	34.03 ± 3.40	–
10	< 10	–	< 10	–	**36**	22.23 ± 0.47	–	< 10	–
11	56.66 ± 5.23	–	< 10	–	**37**	80.53 ± 1.24	2.33 ± 0.86	83.56 ± 2.29	19.85 ± 1.65
12	38.36 ± 1.53	–	< 10	–	**38**	79.43 ± 5.43	1.69 ± 0.74	74.33 ± 2.38	19.50 ± 2.65
13	16.93 ± 1.65	–	< 10	–	**39**	25.24 ± 3.12	–	< 10	–
14	81.10 ± 1.27	6.67 ± 1.52	87.76 ± 2.20	12.76 ± 2.09	**40**	68.29 ± 0.27	7.23 ± 0.98	< 10	–
15	24.37 ± 4.58	–	< 10	–	**41**	28.00 ± 1.31	–	< 10	–
16	39.95 ± 4.91	–	< 10	–	**42**	60.55 ± 2.20	7.67 ± 1.42	55.08 ± 4.85	–
17	< 10	–	< 10	–	**43**	74.47 ± 2.30	2.89 ± 0.33	56.78 ± 0.84	–
18	12.55 ± 2.13	–	< 10	–	**44**	80.90 ± 3.48	1.56 ± 0.31	73.71 ± 2.76	6.88 ± 1.38
19	65.25 ± 5.44	7.19 ± 1.76	43.30 ± 4.32	–	**45**	< 10	–	< 10	–
20	< 10	–	< 10	–	**46**	14.05 ± 3.87	–	< 10	–
21	30.18 ± 2.11	–	< 10	–	**47**	72.08 ± 4.70	4.52 ± 0.30	51.81 ± 2.95	–
22	83.52 ± 2.95	5.82 ± 0.89	86.71 ± 1.73	3.65 ± 0.84	**48**	55.35 ± 1.31	–	47.97 ± 1.99	–
23	34.48 ± 5.55	–	< 10	–	**49**	31.62 ± 0.52	–	< 10	–
24	< 10	–	< 10	–	**50**	78.12 ± 3.78	2.45 ± 0.62	70.49 ± 5.08	20.66 ± 0.84
25	82.72 ± 1.68	6.59 ± 0.72	86.14 ± 4.07	13.15 ± 2.32	Dex	92.13 ± 2.55	–	92.99 ± 3.41	–
26	48.10 ± 5.17	–	< 10	–					

IR, Inhibitory rate.

hanced cell viability compared to the model group. Furthermore, 21 compounds (**5**–**7**, **10**, **12**, **14**, **17**, **19**, **20**, **22**, **23**, **25**, **26**, **33**–**35**, **37**, **38**, **40**, **44**, and **48**) exhibited superior protective effects compared to the positive controls, silymarin and ammonium glycyrrhetate (GA). Six triterpenoids (**10**, **12**, **19**, **22**, **25**, and **48**) demonstrated remarkable protective effects, restoring cell viability to levels comparable to the blank control group. Notably, compounds **19**, **22** and **25** exhibited dual potent activities in both anti-inflammatory and hepatoprotective effects, highlighting their potential as templates for new bioactive molecules.

In conclusion, *G. barbata*, a traditional Mongolian medicine, demonstrates significant medicinal value. The abundant triterpenoid metabolites from *G. barbata* (and the broader Gentianaceae family) remained largely unexplored until now. This study identified 50 triterpenoids (including nine novel compounds) comprising 15 different skeletal structures from the whole plant of *G. barbata*. Compounds **1** and **2** represent a previously undescribed novel framework. The majority of these triterpenoids demonstrated significant anti-inflammatory and hepatoprotective activities. These findings validate the traditional applications of the plant while suggesting potential therapeutic applications of its triterpenoids as anti-inflammatory and hepatoprotective agents, thereby expanding opportunities for its future utilization.

3. Experimental

3.1. General experimental procedures

Column chromatography (CC) was conducted on silica gel (200–300 mesh, Qingdao Marine Chemical Factory, Qingdao, China), neutral Al_2O_3 (200–300 mesh, Shanghai Titan Scientific Co., Ltd., Shanghai, China), Sephadex LH-20 (20–100 μm, Amersham Pharmacia Biotech, Sweden), and MCI gel CHP-20P (70–150 μm, Mitsubishi Chemical Corp., Tokyo, Japan). Thin-layer chromatography (TLC) was performed on silica gel (GF_{254}, 10–40 μm, Qingdao Marine Chemical Factory). TLC spots were

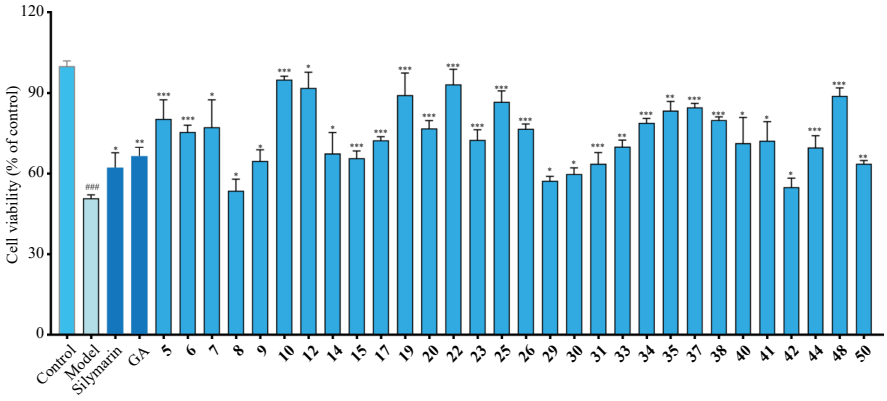

Fig. 5 Hepatoprotective effect of compounds on *t*-BHP-induced hepatotoxicity in HepG2 cells (20 μmol·L^{-1}). Values (mean ± SD, n = 3) are presented as percentage of the mean compared to control.

visualized under UV light or by heating after spraying with 5% H_2SO_4 in EtOH (*V*/*V*). Semipreparative high performance liquid chromatography (HPLC) was performed using an Agilent 1260 series instrument with a Zorbax SB-C_{18} column (5 μm, 9.4 mm × 250 mm, 3 mL·min^{-1}). NMR experiments were conducted using either a Bruker AvanceNeo-600 or AvanceNeo-700 spectrometer with TMS as the internal standard. Mass spectra were acquired on a Waters Synapt XS or an Agilent G6230 spectrometer. ECD and UV spectra were measured on a Chirascan qCD spectrograph. Optical rotations were determined on an Autopol-I spectropolarimeter. X-ray analysis was performed with a Bruker SMART APEX CCD crystallography system.

3.2. Plant materials

The whole plants of *G. barbata* (Froel.) Ma (Gentianaceae) were collected from Lijiang, Yunnan of China (26°52′50.30″N and 100°13′28.40″E) in October 2019, and identified by Wenqing He from Kunming Caizhi Biotechnology Co., Ltd. A voucher specimen (Gb-2019-10) was deposited in the Innovative Institute of Chinese Medicine and Pharmacy, Chengdu University of Traditional Chinese Medicine.

3.3. Extraction and isolation

Dried whole plants of *G. barbata* (5.0 kg) were ground and extracted with menthol (30.0 L × 4) at room temperature. The extracts were concentrated under reduced pressure to yield an oily residue (510.0 g). The residue underwent silica gel CC elution, first with PE followed by a CH_2Cl_2/Me_2CO stepwise-gradient system (from 10∶0 to 0∶10, *V*/*V*), yielding seven fractions (Fr. 1–Fr. 7). Fr. 1 (25.0 g) underwent repeated silica gel CC with PE/CH_2Cl_2 (12∶1, *V*/*V*) as eluent, producing ten subfractions (Fr. 1-1–Fr. 1-10), along with **50** (2.9 mg), **18** (1.9 mg), and **13** (1.1 mg). Fr. 1-4 (2.8 g) was fractionated by Sephadex LH-20 CC using CH_2Cl_2/MeOH (1∶1, *V*/*V*) to yield two subfractions (Fr. 1-4-1–Fr. 1-4-2). Fr. 1-4-1 (730.0 mg) was purified through Al_2O_3 CC using PE/CH2Cl2 (15∶1, *V*/*V*) to obtain **40** (3.5 mg). Fr. 1-5 (3.2 g) was separated *via* Sephadex LH-20 CC with CH_2Cl_2/MeOH (1∶1, *V*/*V*) to produce two subfractions (Fr. 1-5-1–Fr. 1-5-2). Fr. 1-5-1 (180.0 mg) underwent Al_2O_3 CC purification using PE/CH_2Cl_2 (15∶1, *V*/*V*) to yield **1** (8.5 mg) and **2** (0.9 mg). Fr. 1-5-2 (380.0 mg) underwent silica gel CC with PE/CH_2Cl_2 (15∶1, *V*/*V*) to yield **30** (177.0 mg). Fr. 1-6 (3.0 g) was fractionated through Sephadex LH-20 CC using CH_2Cl_2/MeOH (1∶1, *V*/*V*) to give two subfractions (Fr. 1-6-1–Fr. 1-6-2). Fr. 1-6-2 (53.1 mg) was purified *via* Al_2O_3 CC with PE/CH_2Cl_2 (15∶1, *V*/*V*) to yield **3** (37.1 mg). Fr. 1-6-3 (47.1 mg) underwent semi-preparative RP-HPLC using CH_3OH–H_2O (100∶0, *V*/*V*) as mobile phase to yield **45** (t_R 23.6 min, 15.2 mg), **23** (t_R 26.3 min, 11.5 mg), and **8** (t_R 28.3 min, 5.0 mg). Fr. 1-7 (177.1 mg) underwent silica gel CC with PE/CH_2Cl_2 (20∶1, *V*/*V*), followed by Sephadex LH-20 CC using CH_2Cl_2/MeOH (1∶1, *V*/*V*) to produce three subfractions (Fr. 1-7-1–Fr. 1-7-3). Fr. 1-7-2 (12.0 mg) underwent semi-preparative RP-HPLC using CH_3OH–H_2O (95∶5, *V*/*V*) as mobile phase to yield **21** (t_R 10.6 min, 0.4 mg), **12** (t_R 10.9 min, 1.2 mg), **49** (t_R 11.4 min, 1.7 mg), and **22** (t_R 13.6 min, 0.8 mg). Fr. 1-7-3 (8.0 mg) underwent semi-preparative RP-HPLC using CH_3OH–H_2O (95∶5, *V*/*V*) as mobile phase to yield **36** (t_R 11.6 min, 0.8 mg) and **38** (t_R 12.2 min, 2.0 mg). Fr. 1-9 (8.7 mg) was purified through Sephadex LH-20 CC with CH_2Cl_2/MeOH (1∶1, *V*/*V*), then underwent semi-preparative RP-HPLC using CH_3OH–H_2O (95∶5, *V*/*V*) as mobile phase to yield **20** (t_R 23.6 min, 5.0 mg) and **37** (t_R 25.8 min, 1.0 mg). Fr. 2 (27.0 g) underwent MCI gel CC with a MeOH/H_2O stepwise-gradient system (from 6∶4 to 10∶0, *V*/*V*) to give five subfractions (Fr. 2-1–Fr. 2-5). Fr. 2-5 (7.0 g) was purified *via* Al_2O_3 CC using PE/acetone (15∶1, *V*/*V*), followed by Sephadex LH-20 CC with CH_2Cl_2/MeOH (1∶1, *V*/*V*) to produce six subfractions (Fr. 2-5-1–Fr. 2-5-6). Fr. 2-5-3 (11 mg) was further subjected to semi-preparative RP-HPLC using MeCN–H_2O (90∶10, *V*/*V*) as the mobile phase to yield **29** (t_R 15.2 min, 0.7 mg), **11** (t_R 30.0 min, 2.6 mg), and **44** (t_R 20.3 min, 0.6 mg). Fr. 2-5-4 (27.0 mg) was purified by semi-preparative RP-HPLC using MeCN/H_2O (85∶15, *V*/*V*) as the mobile phase to yield **10** (t_R 8.4 min, 6.7 mg), **47** (t_R 15.4 min, 1.8 mg), **16** (t_R 17.7 min, 1.8 mg), **28** (t_R 18.7 min, 0.2 mg), and **32** (t_R 21.0 min, 11.6 mg). Fr. 2-5-5 (135.0 mg) was applied to semi-preparative RP-HPLC using MeCN–H_2O (80∶20, *V*/*V*) as the mobile phase to yield **5** (t_R 13.6 min, 82.2 mg). Fr. 2-5-6 (27.0 mg) was separated by semi-preparative RP-HPLC using MeCN/H_2O (75∶25, *V*/*V*) as the mobile phase to yield **33** (t_R 12.7 min, 6.0 mg) and **4** (t_R 22.6 min, 9.3 mg). Fr. 3 (30.0 g) was applied to MCI gel CC eluted with a MeOH/H_2O stepwise-gradient system (from 6∶4 to 10∶0, *V*/*V*) to give three subfractions (Fr. 3-1–Fr. 3-3). Fr. 3-3 (8.0 g) was purified by Sephadex LH-20 CC eluting with CH_2Cl_2/MeOH (1∶1, *V*/*V*) to obtain two subfractions (Fr. 3-3-1–Fr. 3-3-2). Fr. 3-3-1 (13.0 mg) was successively purified over Al_2O_3 and silica gel CC eluting with PE/acetone (10∶1, *V*/*V*) to yield **46** (3.0 mg), **19** (3.0 mg), and **9** (1.2 mg). Fr. 3-3-2 (57.0 g) was applied to semi-preparative RP-HPLC using CH_3OH/H_2O (85∶15, *V*/*V*) as the mobile phase to yield **24** (t_R 20.7 min, 21.0 mg) and **35** (t_R 21.7 min, 8.7 mg). Fr. 4 (15.0 g) was applied to MCI gel CC eluted with a MeOH/H_2O stepwise-gradient system (from 6∶4 to 10∶0, *V*/*V*) to give four subfractions (Fr. 4-1–Fr. 4-4). Fr. 4-4 (2.8 g) was subjected to silica gel CC eluting with PE/acetone (6∶1, *V*/*V*), and then to Sephadex LH-20 CC with CH_2Cl_2/MeOH (1∶1, *V*/*V*) as the eluent to give two subfractions (Fr. 4-4-1–Fr. 4-4-2). Fr. 4-4-1 (5.4 mg) was applied to semi-preparative RP-HPLC using MeCN/H_2O (90∶10, *V*/*V*) as the mobile phase to yield **34** (t_R 22.1 min, 1.4 mg). Fr. 4-4-2 (23.0 mg) was separated by semi-preparative RP-HPLC using MeCN/H_2O (90∶10, *V*/*V*) as the mobile phase to yield

48 (t_R 10.5 min, 0.7 mg), **7** (t_R 13.47 min, 0.7 mg), **14** (t_R 14.47 min, 0.2 mg), **15** (t_R 15.4 min, 1.0 mg), **31** (t_R 16.4 min, 0.5 mg), and **6** (t_R 17.6 min, 0.9 mg). Fr. 5 (140.0 g) was applied to MCI gel CC eluted with a MeOH/H_2O stepwise-gradient system (from 6∶4 to 10∶0, *V/V*) to give four subfractions (Fr. 5-1–Fr. 5-4). Fr. 5-2 (108.0 g) was purified by Sephadex LH-20 CC eluting with CH_2Cl_2/MeOH (1∶1, *V/V*), and then by Al_2O_3 CC eluting with PE/acetone (2∶1, *V/V*) to yield **17** (70.0 g). Fr. 6 (45.0 g) was applied to MCI gel CC eluted with a MeOH/H_2O stepwise-gradient system (from 6∶4 to 10∶0, *V/V*) to obtain four subfractions (Fr. 6-1–Fr. 6-4). Fr. 6-4 (17.0 g) was subjected to Al_2O_3 CC eluting with PE/EtOAc (6∶1, *V/V*) to give three subfractions (Fr. 6-4-1–Fr. 6-4-3). Fr. 6-4-3 (22.0 mg) was purified by Sephadex LH-20 CC eluting with CH_2Cl_2/MeOH (1∶1, *V/V*) as the mobile phase to yield **27** (3.7 mg) and **43** (1.6 mg). Fr. 7 (80.0 g) was applied to MCI gel CC eluted with a MeOH/H_2O stepwise-gradient system (from 6∶4 to 10∶0, *V/V*) to give two subfractions (Fr. 7-1–Fr. 7-2). Fr. 7-1 (16.0 g) was applied to silica gel CC eluting with PE/acetone (4∶1, *V/V*), and then to Sephadex LH-20 CC eluting with CH_2Cl_2/MeOH (1∶1, *V/V*) to give three subfractions (Fr. 7-1-1–Fr. 7-1-3). Fr. 7-1-2 (3.8 mg) was purified by semi-preparative RP-HPLC using MeCN/H_2O (75∶25, *V/V*) as the mobile phase to yield **41** (t_R 12.0 min, 1.5 mg) and **25** (t_R 24.0 min, 0.6 mg). Fr. 7-2 (23.0 g) was subjected to silica gel CC with PE/acetone (7∶1, *V/V*), and then to Sephadex LH-20 CC with CH_2Cl_2/MeOH (1∶1, *V/V*) as the eluent to obtain two subfractions (Fr. 7-2-1–Fr. 7-2-2). Fr. 7-2-2 (23.1 mg) was purified by semi-preparative RP-HPLC using MeCN/H_2O (75∶25, *V/V*) as the mobile phase to yield **26** (t_R 19.3 min, 4.8 mg) and **42** (t_R 20.5 min, 10.5 mg).

Gentianopsolide A (***1***). White powder; $[\alpha]_D^{20}$ +12.5 (*c* 0.10, MeOH); ^{1}H and ^{13}C NMR data, see Tables 1 and 2; HR-ESI-MS *mz* 479.3861 $[M + Na]^+$ (Calcd. for $C_{31}H_{52}O_2Na$, 479.3860).

Gentianopsolide B (***2***). White powder; $[\alpha]_D^{20}$ −8.4 (*c* 0.10, MeOH); ^{1}H and ^{13}C NMR data, see Tables 1 and 2; HR-ESI-MS *m/z* 455.3885 $[M + H]^+$ (Calcd. for $C_{31}H_{51}O_2$, 455.3889).

Crystal data for 3-oxo-24-methylenecycloarane (***3***). $C_{31}H_{50}O$, *Mr* = 438.71, *a* = 12.3745(14) Å, *b* = 7.2213(8) Å, *c* = 59.844(7) Å, *α* = 90°, *β* = 91.375(4)°, *γ* = 90°, *V* = 5346.1(10) Å^3, *T* = 150.(2) K, space group *C*121, *Z* = 8, *μ*(Cu Kα) = 0.467 mm^{-1}, 13647 reflections measured, 7918 independent reflections (R_{int} = 0.0815). The final R_1 values were 0.2130 ($I > 2\sigma(I)$). The final $wR(F^2)$ values were 0.5149 ($I > 2\sigma(I)$). The final R_1 values were 0.2198 (all data). The final $wR(F^2)$ values were 0.5244 (all data). The goodness of fit on F^2 was 2.340. Flack parameter = 0.9(4). The crystallographic data in standard CIF format were deposited at the Cambridge Crystallographic Data Centre (CCDC 2381310).

17β-Hydroperoxide olean-13(18)-en-3β-ol (***7***). White powder; $[\alpha]_D^{20}$ +13.5 (*c* 0.10, MeOH); ^{1}H and ^{13}C NMR data, see Tables 1 and 2; HR-EI-MS *m/z* 444.3597 $[M]^+$ (Calcd. for $C_{29}H_{48}O_3$, 444.3598).

28-Nor-olean-18-en-3β,17β-diol (***10***). White powder; $[\alpha]_D^{20}$ −16.8 (*c* 0.10, MeOH); ^{1}H and ^{13}C NMR data, see Tables 1 and 2; HR-ESI-MS *m/z* 451.3548 $[M + Na]^+$ (Calcd. for $C_{29}H_{48}O_2Na$, 451.3547).

3β-Palmitoyl-28-nor-olean-12-en-17β-ol (***20***). White powder; $[\alpha]_D^{20}$ +53.7 (*c* 0.10, MeOH); ^{1}H and ^{13}C NMR data, see Tables 1 and 3; HR-ESI-MS *m/z* 689.5836 $[M + Na]^+$ (Calcd. for $C_{45}H_{78}O_3Na$, 689.5849).

Gentianopsolide C (***28***). White powder; $[\alpha]_D^{20}$ +18.6 (*c* 0.10, MeOH); ^{1}H and ^{13}C NMR data, see Tables 1 and 3; HR-EI-MS *m/z* 470.3756 $[M]^+$ (Calcd. for $C_{31}H_{50}O_3$, 470.3754).

Gentianopsolide D (***29***). White powder; $[\alpha]_D^{20}$ −75.0 (*c* 0.10, MeOH); ^{1}H and ^{13}C NMR data, see Tables 1 and 3; HR-EI-MS *m/z* 456.3597 $[M]^+$ (Calcd. for $C_{30}H_{48}O_3$, 456.3598).

3β-Palmitoyl-28-nor-urs-12-en-17β-ol (***37***). Colorless oil; $[\alpha]_D^{20}$ +50.1 (*c* 0.10, MeOH); ^{1}H and ^{13}C NMR data, see Tables 1 and 3. HR-ESI-MS *m/z* 667.6043 $[M + H]^+$ (Calcd. for $C_{45}H_{79}O_3$, 667.6029).

Urs-20(30)-en-3β,21α-diol-28-oic acid (***41***). White powder; $[\alpha]_D^{20}$ −9.2 (*c* 0.10, MeOH); ^{1}H and ^{13}C NMR data, see Tables 1 and 2; HR-ESI-MS *m/z* 471.3484 $[M - H]^-$ (Calcd. for $C_{30}H_{47}O_4$, 471.3474).

3.4. Quantum chemistry computations

The conformational analysis was conducted using the Spartan 14 software package with MMFF minimization force field. The resulting conformers underwent further optimization using Gaussian 09 software through density functional theory (DFT) calculations at the B3LYP/6-31 + G (d, p) level *in vacuum*. Conformations with Boltzmann distributions of Gibbs free energies exceeding 1% were subsequently utilized for NMR calculations using the GIAO method at the MPW1PW91/6-311 + G (d, p) level, or ECD calculations using the TD-DFT method with basis set CAM-B3LYP/DGDZVP. The ECD spectra of various conformers were simulated using a Gaussian function with a half-bandwidth ranging from 0.12 to 0.40 eV. The comprehensive theoretical ECD spectra were generated according to the Boltzmann weighting and simulated experimental spectra using the SpecDis software. Additional details were provided in the supplemental material.

3.5. Anti-inflammatory assay

Anti-inflammatory assay was conducted following previous reports [34–36]. RAW 264.7 cells were seeded in a 96-well plate at a density of 2 × 10^4 cells/well for 24 h maintained in Dulbecco's modified Eagle's medium (DMEM) containing 10% fetal bovine serum (FBS), 1% penicillin and 1% streptomycin, followed by treatment with compounds at 20 μmol·L^{-1}. Dexamethasone (Dex, Solarbio) served as a positive control. After 1 h, cells were stimulated with LPS (1 μg·mL^{-1}) (Beyotime Biotechnology) for 24 h. Subsequently, 10 μL of cell counting kit-8 (CCK-8) (Bioground) was added to each well to assess cell viability. Following 30 min of incubation, the optical density at 450 nm was measured using a microplate reader (Molecular Devices). Cytokine levels (TNF-α and IL-6) in cell supernatant were determined using enzyme-linked immunosorbent assay (ELISA) kits according to manufacturer's instructions. Compounds demonstrating superior inhibition rates (> 60%) at 20 μmol·L^{-1} were selected for IC_{50} value determination at varying concentrations. All experiments were performed in triplicate.

3.6. Hepatoprotective assay

The hepatoprotective assay was conducted according to previous reports with minor modifications [33, 37]. HepG2 cells were seeded in a 96-well plate at a density of 5 × 10^4 cells/well for 24 h maintained in DMEM containing 10% FBS, 0.5% penicillin, and 0.5% streptomycin, followed by treatment with compounds at 20 μmol·L^{-1} for 2 h. Silymarin and ammonium GA served as positive controls. *t*-BHP was subsequently added to achieve a final concentration of 250 μmol·L^{-1} and the solutions were incubated for 2.5 h. Subsequently, 10 μL of CCK-8 (Bioground) was added to each well to assess cell viability. After 30 min of incubation, the optical density at 450 nm was measured using a microplate reader (Molecular Devices).

Funding

This work was supported by the National Natural Science Foundation of China (Nos. 21937006, U23A20510, 82204245, 82222072, and U24A20806), the Strategic Priority Research Program of the Chinese Academy of Sciences (No. XDB1230000), and the Research Project of Yunnan Province (Nos. 202401BC070016 and 202402AA310047).

Supporting information

The 1D and 2D NMR and HRMS spectra of new compounds, and details of quantum chemical calculations are available as Supporting Information, and can be requested by sending E-mail to the corresponding authors.

Declaration of competing interest

These authors have no conflict of interest to declare.

References

1 Li Y, Wang J, Li L, et al. Natural products of pentacyclic triterpenoids: from discovery to heterologous biosynthesis. *Nat Prod Rep*. 2023;40:1303-1353. https://doi.org/10.1039/D2NP00063F.
2 Guinda A, Rada M, Delgado T, et al. Pentacyclic triterpenoids from olive fruit and leaf. *J Agric Food Chem*. 2010;58(17):9685-9691. https://doi.org/10.1021/jf102039t.
3 Liu ZQ. Chemical insights into ginseng as a resource for natural antioxidants. *Chem Rev*. 2012;112(6):3329-3355. https://doi.org/10.1021/cr100174k.
4 Salvador JAR, Moreira VM, Goncalves BMF, et al. Ursane-type pentacyclic triterpenoids as useful platforms to discover anticancer drugs. *Nat Prod Rep*. 2012;29:1463-1479. https://doi.org/10.1039/c2np20060k.
5 Topçu G. Bioactive triterpenoids from *Salvia* species. *J Nat Prod*. 2006;69:482-487. https://doi.org/10.1021/np0600402.
6 Feng Z, Zheng Y, Jiang Y, et al. Complete chloroplast genome of *Gentianopsis barbata* and comparative analysis with related species from Gentianaceae. *Genome*. 2022;65(7):363-375. https://doi.org/10.1139/gen-2021-0080.
7 Cui ZH, Li Y, Wang ZW, et al. Chemical constituents from *Gentianopsis barbata* var. *sinensis* Ma (Gentianaceae). *Biochem Syst Ecol*. 2013;47:101-103. https://doi.org/10.1016/j.bse.2012.11.003.
8 Xi G, Wang T, Bao G, et al. Chemical constituents from *Gentianopsis barbata*. *Chin Tradit Pat Med*. 2022;44(6):1850-1854. https://doi.org/10.3969/j.issn.1001-1528.2022.06.022.
9 Ferreira MDL, Fernandes DA, Nunes FC, et al. Phytochemical study of *Waltheria viscosissima* and evaluation of its larvicidal activity against *Aedes aegypti*. *Rev Bras Farmacogn*. 2019;29(5):582-590. https://doi.org/10.1016/j.bjp.2019.05.008.
10 Ikeda Y, Sugiura M, Fukaya C, et al. Periandradulcins A, B and C: phosphodiesterase inhibitors from *Periandra dulcis* Mart. *Chem Pharm Bull*. 1991;39(3):566-571. https://doi.org/10.1248/cpb.39.566.
11 Ikuta A, Morikawa A. Triterpenes from *Stauntonia hexaphylla* callus tissues. *J Nat Prod*. 1992;55(9):1230-1233. https://doi.org/10.1021/np50087a008.
12 Tanaka R, Ida T, Takaoka Y, et al. 3,4-*Seco*-oleana-4(23),18-dien-3-oic acid and other triterpenes from *Euphorbia chamaesyce*. *Phytochemistry*. 1994;36(1):129-132. https://doi.org/10.1016/S0031-9422(00)97025-0.
13 Benyahia S, Benayache S, Benayache F, et al. Cladocalol, a pentacyclic 28-*nor*-triterpene from *Eucalyptus cladocalyx* with cytotoxic activity. *Phytochemistry*. 2005;66(6):627-632. https://doi.org/10.1016/j.phytochem.2004.12.018.
14 Ames TR, Beton JL, Bowers A, *et al*. The chemistry of the triterpenes and related compounds. Part XXIII. The structure of taraxasterol, ψ-taraxasterol (heterolupeol), and lupenol-I. *J Chem Soc*. 1954:1905-1919. https://doi.org/10.1039/jr9540001902.
15 Alves JS, Castro JCM, Freire MO, et al. Complete assignment of the ^{1}H and ^{13}C NMR spectra of four triterpenes of the ursane, artane, lupane and friedelane groups. *Magn Reson Chem*. 2000;38(3):201-206. https://doi.org/10.1002/(SICI)1097-458X(200003)38:3<201::AID-MRC622>3.0.CO;2-0.
16 Pinto CA, Baker PM, Gilbert B, et al. Vellozone, a tetracyclic triterpene from *Vellozia stipitata*. *Phytochemistry*. 1980;19(11):2486-2487. https://doi.org/10.1016/S0031-9422(00)91063-X.
17 Mai HL, Grellier P, Prost E, et al. Triterpenes from the exudate of *Gardenia urvillei*. *Phytochemistry*. 2016;122:193-202. https://doi.org/10.1016/j.phytochem.2015.11.001.
18 Zhong HT, Li F, Chen B, et al. Euphane triterpenes from the bark of *Broussonetia papyrifera*. *Helv Chim Acta*. 2011;94(11):2061-2065. https://doi.org/10.1002/hlca.201100136.
19 Niu XF, Liu X, Pan L, et al. Oleanene triterpenes from *Sedum lineare* Thunb. *Fitoterapia*. 2011;82(7):960-963. https://doi.org/10.1016/j.fitote.2011.05.011.
20 Marner FJ, Freyer A, Lex J. Triterpenoids from gum mastic, the resin of *Pistacia lentiscus*. *Phytochemistry*. 1991;30(11):3709-3712. https://doi.org/10.1016/0031-9422(91)80095-I.
21 Ji F, Li ZL, Niu SL, et al. Studies on the chemical constituents of the barks of *Garcinia xanthochymus*. *Chin J Med Chem*. 2012;22:507-510.
22 Cao S, Guza RC, Miller J, et al. Cytotoxic triterpenoids from *Acridocarpus vivy* from the Madagascar rain forest. *J Nat Prod*. 2004;67(6):986-989. https://doi.org/10.1021/np040058h.
23 Takahashi H, Iuchi M, Fujita Y, et al. Coumaroyl triterpenes from *Casuarina equisetifolia*. *Phytochemistry*. 1999;51(4):543-550. https://doi.org/10.1016/S0031-9422(99)00070-9.
24 Huang Y, Aisa HA, Isaev MI. Isoprenoids of *Euphorbia sororia*. I. Triterpenoids. *Chem Nat Comp*. 2009;45:921-924. https://doi.org/10.1007/s10600-010-9459-y.
25 Seebacher W, Simic N, Weis R, et al. Complete assignments of ^{1}H and ^{13}C NMR resonances of oleanolic acid, 18α-oleanolic acid, ursolic acid and their 11-oxo derivatives. *Magn Reson Chem*. 2003;41(8):636-638. https://doi.org/10.1002/mrc.1214.
26 Mahato SB, Kundu AP. ^{13}C NMR spectra of pentacyclic triterpenoids–a compilation and salient features. *Phytochemistry*. 1994;37(6):1517-1575. https://doi.org/10.1016/S0031-9422(00)89569-2.
27 Ikuta A, Kamiya K, Satakek T, et al. Triterpenoids from callus tissue cultures of *Paeonia species*. *Phytochemistry*. 1995;38(5):1203-1207. https://doi.org/10.1016/0031-9422(94)00445-Y.
28 Merfort I, Buddrus J, Nawwar MAM, et al. A triterpene from the bark of *Tamarix aphylla*. *Phytochemistry*. 1992;1(11):4031-4032. https://doi.org/10.1016/S0031-9422(00)97580-0.
29 Khalilov LM, Khalilova AZ, Shakurova ER, et al. PMR and ^{13}C NMR spectra of biologically active compounds. XII. Taraxasterol and its acetate from the aerial part of *Onopordum acanthium*. *Chem Nat Comp*. 2003;39:285-288. https://doi.org/10.1023/A:1025478720459.
30 Tanaka N, Duan H, Takaishi Y, et al. Terpenoids from *Tripterygium doianum* (Celastraceae). *Phytochemistry*. 2002;61(1):93-98. https://doi.org/10.1016/S0031-9422(02)00219-4.
31 Yamashita H, Matsuzaki M, Kurokawa Y, et al. Four new triterpenoids from the bark of *Euonymus alatus* forma *ciliato-dentatus*. *Phytochem Lett*. 2019;31:140-146. https://doi.org/10.1016/j.phytol.2019.03.015.
32 Tanaka H, Noguchi H, Abe I. 1-Methylidenesqualene and 25-methylidenesqualene as active-site probes for bacterial squalene: hopene cyclase. *Org Lett*. 2004;6(5):803-806. https://doi.org/10.1021/ol036509r.
33 Long L, Yang Y, Zhu T, et al. New pentacyclic triterpenoids isolated from *Leptopus chinensis* and their hepatoprotective activities on *tert*-butyl hydroperoxide-induced oxidative injury. *RSC Adv*. 2021;11(21):12784-12793. https://doi.org/10.1039/D1RA00962A.
34 Guo K, Zhou TT, Luo SH, et al. Leucosceptrane sesterterpenoids as a new type of natural immunosuppressive agents in treating sepsis. *J Med Chem*. 2024;67(1):513-528. https://doi.org/10.1021/acs.jmedchem.3c01759.
35 Chen YG, Li DS, Ling Y, et al. A cryptic plant terpene cyclase producing unconventional 18- and 14-membered macrocyclic C_{25} and C_{20} terpenoids with immunosuppressive activity. *Angew Chem Int Ed*. 2021;133(48):25672-25680. https://doi.org/10.1002/ange.202110842.
36 Chen LZ, Sun WW, Bo L, et al. New arylpyrazoline-coumarins: synthesis and anti-inflammatory activity. *Eur J Med Chem*. 2017;138:170-181. https://doi.org/10.1016/j.ejmech.2017.06.044.
37 Li B, Bo S, Sheng Z, et al. Hepatoprotective activity and mechanisms of prenylated stilbenoids. *J Agric Food Chem*. 2024;72(3):1618-1629. https://doi.org/10.1021/acs.jafc.3c09515.